

# Planar tetra-coordinate carbon resulting in enhanced third-order nonlinear optical response of metal-terminated graphene nanoribbons

Guo-Liang Chai <sup>a,b</sup>, Chen-Sheng Lin <sup>a</sup> and Wen-Dan Cheng <sup>\*a</sup>

<sup>a</sup> State Key Laboratory of Structural Chemistry, Fujian Institute of Research on the Structure of Matter, Chinese Academy of Sciences, Fuzhou, Fujian 350002, China; and Fujian Provincial Key Laboratory of Theoretical and Computational Chemistry, Fuzhou, Fujian 350002, China.

<sup>b</sup> Graduate School of the Chinese Academy of Sciences, Beijing, 100039, P. R. China.

\*E-mail: [cwd@fjirsm.ac.cn](mailto:cwd@fjirsm.ac.cn)

## 1. The detailed equations used for the calculation of nonlinear reflectivity

The nonlinear reflectivity R can be expressed as:

$$R = \tan^2[|\gamma'| l] \quad (1)$$

Where  $l$  is the length of device (0.2cm is used in this study);  $\gamma'$  is coupling coefficient which can be written as:

$$\gamma' = \frac{\omega}{2cn_0(\omega)} \chi^{(3)} A^2 \quad (2)$$

Here,  $\omega$ ,  $n_0$  and  $A$  are frequency, refractive index and real amplitude functions of plane pump waves, respectively. The power of laser is related to  $A$ :

$$I = \frac{1}{2} \epsilon_0 n_0(\omega) c A^2 \quad (3)$$

In this paper, we set  $I=10^{12} \text{ W.m}^{-2}$ . Third-order optical susceptibilities  $\chi^{(3)}$  of bulk materials can be estimated from the average third-order polarizability  $\langle \gamma \rangle$ :

$$\chi^{(3)}(-\omega_p; \omega_1, \omega_2, \omega_3) = N f(\omega_1) f(\omega_2) f(\omega_3) f(\omega_p) \langle \gamma \rangle \quad (4)$$

and the local field factor  $f(\omega_i)$  is expressed as:

$$f(\omega_i) = [n(\omega_i)^2 + 2]/3 = 1/[1 - (4\pi/3)N\alpha(\omega_i)] \quad (5)$$

where  $f(\omega_i)$  is at radiation frequency  $\omega_i$ ,  $N$  is the dimmer number density (The distance between GNRs is about 0.34nm. According to the size of studied materials, we set the  $N$  to be  $1.56 \times 10^{27} \text{ m}^{-3}$ ), and  $n(\omega_i)$  and  $\alpha(\omega_i)$  are the refractive index and the polarizability, respectively, and can also be obtained by the TDDFT-SOS method.

After the  $n(\omega_i)$ ,  $A$ , and  $\chi^{(3)}(-\omega_p; \omega_1, \omega_2, \omega_3)$  have been calculated, we will obtain the dynamic (under different input photon energy  $\hbar\omega_i$ ) nonlinear reflectivity  $R$ .

## 2. Supporting figures

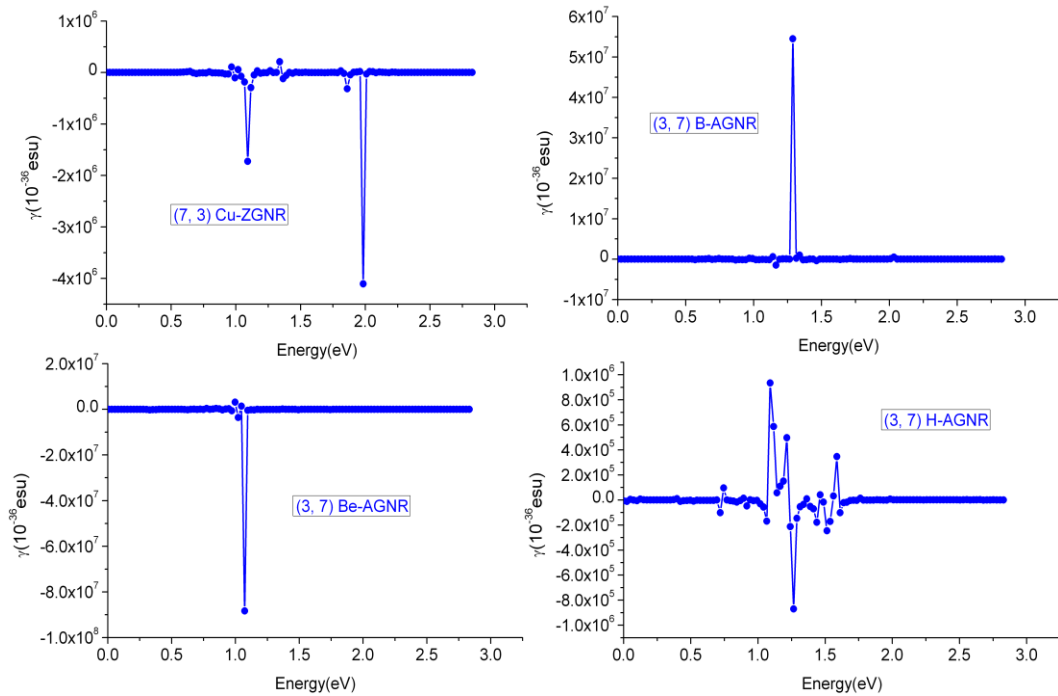


**Figure S1.** The dynamic third order NLO polarizabilities (polarizabilities under different input photon energy) for THG process.

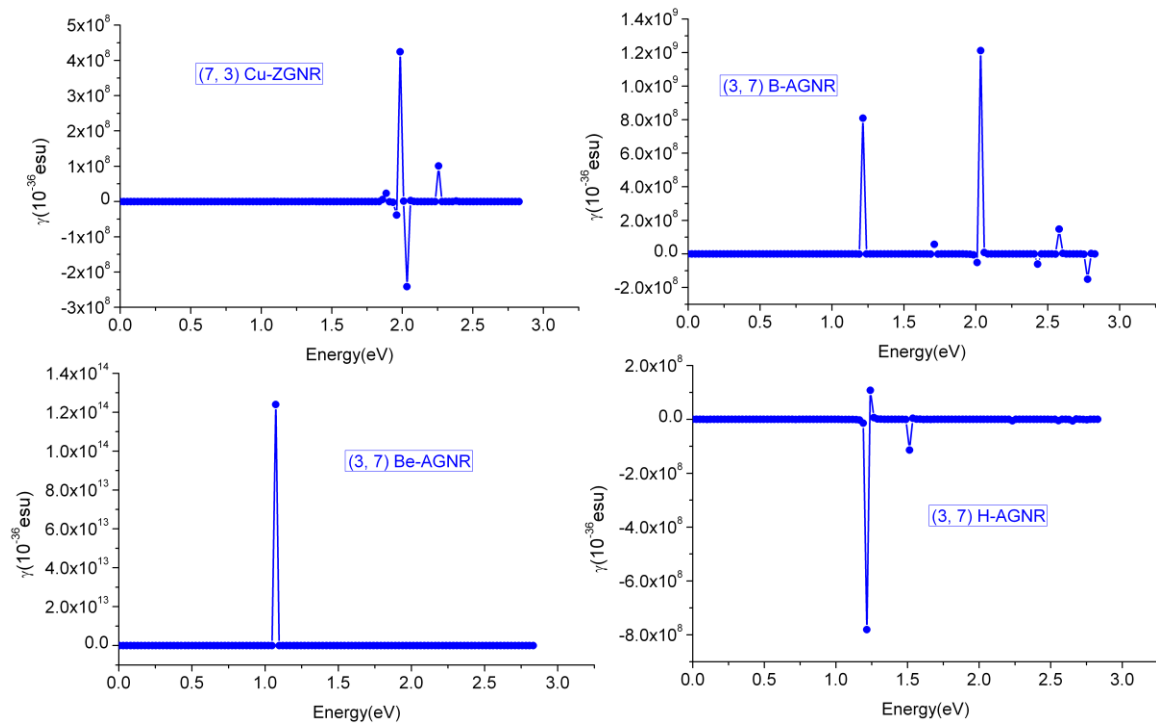


**Figure S2.** The dynamic third order NLO polarizabilities (polarizabilities under different input photon energy) for DFWM process.

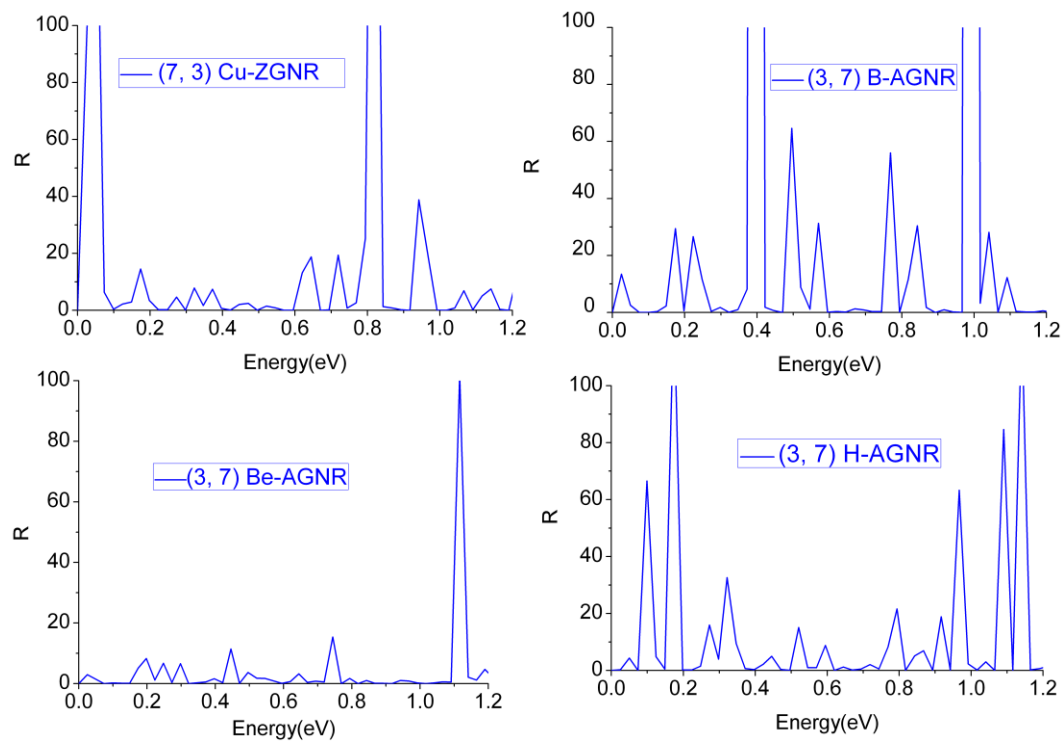


**Figure S3.** Dynamic nonlinear reflectivity ( $R$  value under different input photon energy) of (a)  $(7, 3)$  Cu-ZGNR, (b)  $(3, 7)$  B-AGNR, (c)  $(3, 7)$  Be-AGNR and (d)  $(3, 7)$  H-AGNR.

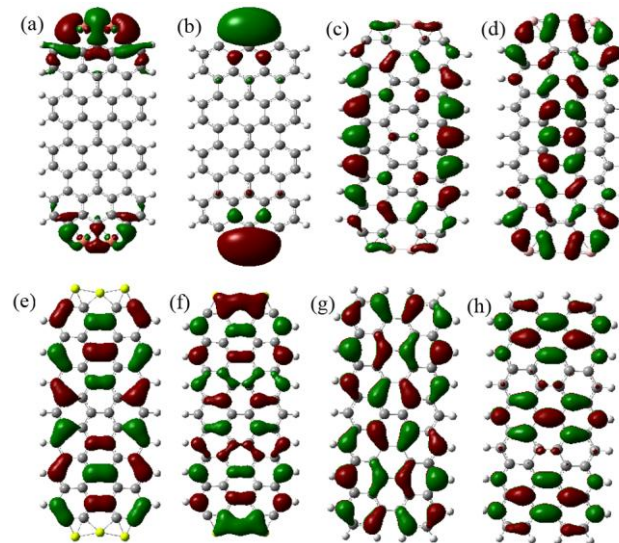


**Figure S4.** The orbital configurations of the most contributed states as described in Table 2. (a) H-5 of  $(7, 3)$  Cu-ZGNR, (b) L+7 of  $(7, 3)$  Cu-ZGNR, (c) H of  $(3, 7)$  B-AGNR, (d) L+16 of  $(3, 7)$  B-AGNR (e) H-7 of  $(3, 7)$  Be-AGNR, (f) L+1 of  $(3, 7)$  Be-AGNR, (g) H of  $(3, 7)$  H-AGNR, (h) L+1 of  $(3, 7)$  H-AGNR.

Be-AGNR, (g) H-1 of (3, 7) H-AGNR, and (h) L+7 of (3, 7) H-AGNR.

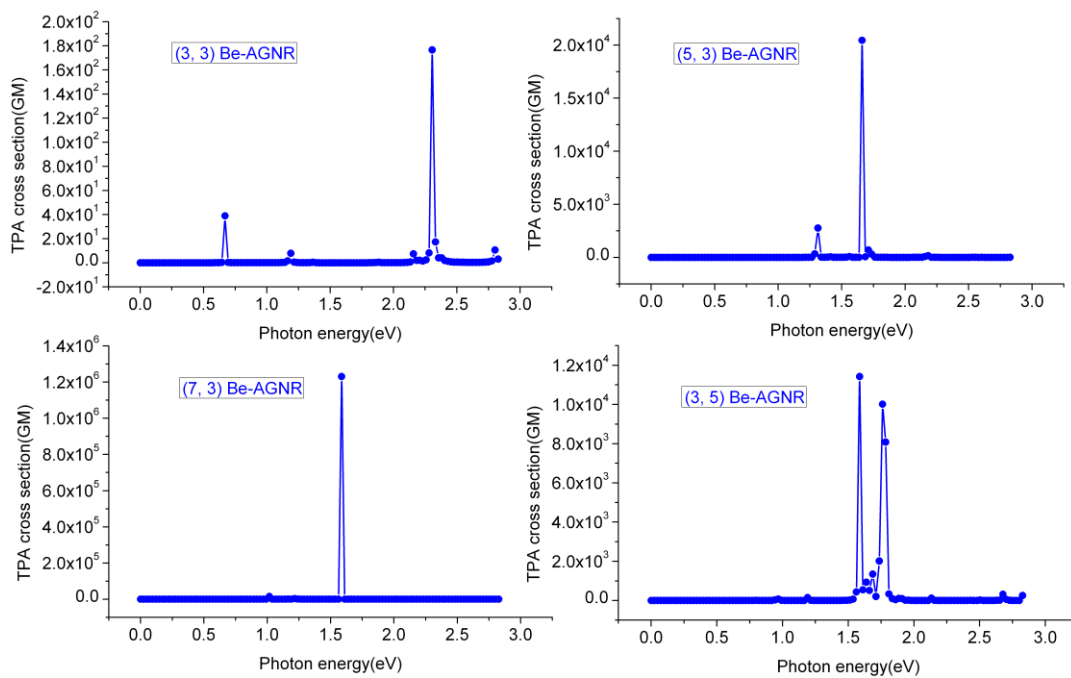


**Figure S5.** Frequency-dependent TPA cross sections of Be-AGNRs.

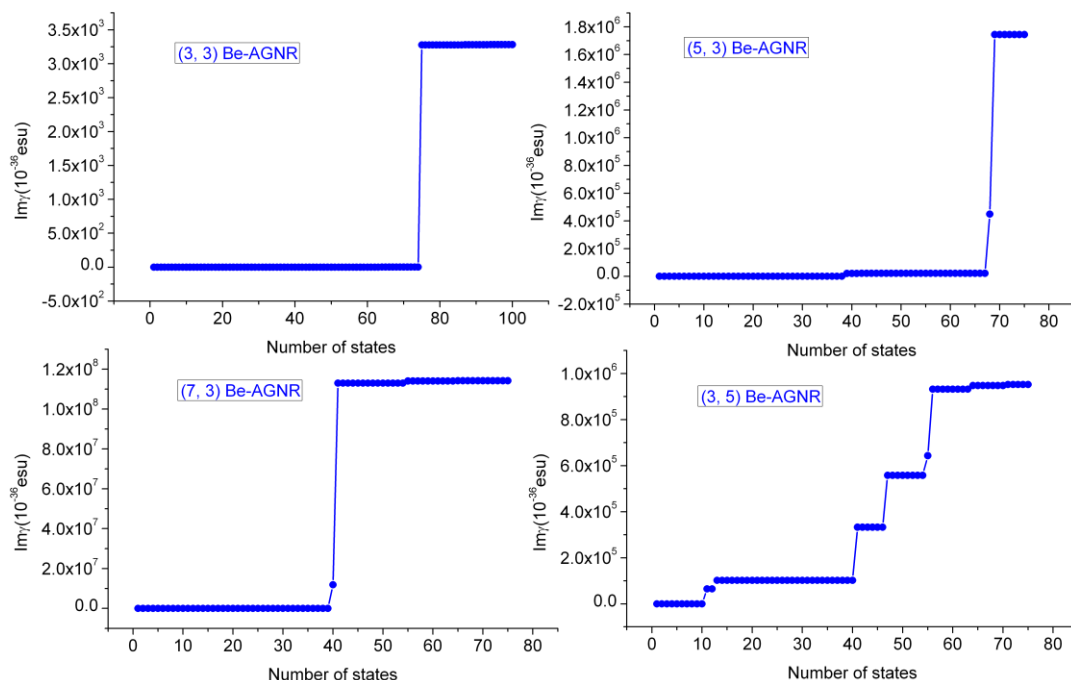


**Figure S6.** The relationship of  $\text{Im}\gamma(-\omega; \omega, \omega, -\omega)$  versus two-photon states at the resonant energy for Be-AGNRs.

